

2 biomass through an alternative view on plot biomass

3 Christoph Kleinn^{1*}, Steen Magnussen³, Nils Nölke¹, Paul Magdon¹, Juan Gabriel
4 Álvarez-González², Lutz Fehrmann¹, César Pérez-Cruzado^{1,2},

5 ¹Forest Inventory and Remote Sensing, Georg-August-Universität Göttingen,
6 D-37077 Göttingen, Germany

7 ²Current address: Department of Agroforestry Engineering, University of Santiago de
8 Compostela, E-27002 Lugo, Spain

9 ³Canadian Forest Service, Natural Resources Canada, Victoria BC, V8Z 1M5, Canada

10
11 * Corresponding author. Tel.: (+49) 551 39 33472

12 E-mail: ckleinn@gwdg.de

13 14 **Keywords:**

15 Branch biomass, foliage biomass, stem biomass, biomass surface plots, sampling surfaces,
16 standard error of estimation

17 18 **Abstract:**

19 We contrast a new continuous approach (CA) to estimation of plot level above-ground biomass
20 (AGB) in forest inventories with the current approach of deriving the AGB estimate exclusively
21 from the tree-level AGB predicted for each tree in a plot; henceforth called DA (discrete
22 approach). In CA the AGB in a forest is modelled as a continuous surface and the AGB estimate
23 for a fixed area plot is computed as the integral of the AGB surface taken over the plot. Hence
24 with CA, the portions of biomass in plot-trees that extend across a plot perimeter is ignored

25 while the biomass from trees outside the plot reaching inside the plot is added. We use a
26 sampling simulation with data from a fully mapped 2 ha area to illustrate, that important
27 differences in plot-level AGB estimates can emerge, and that one should expect CA-based
28 estimates of AGB to be less variable than with the DA, which translates to a higher precision
29 of estimates from field plots: in our case study, for a target precision of estimation of 5%, the
30 required sample size was 27% lower for small plots of 100m² when using the CA and 10%
31 lower for larger plots of 1700m². We discuss practical issues to implementing CA in field
32 inventories and discuss the expected potential for applications that model biomass from remote
33 sensing data.

34

35 **1. Background**

36 Fixed area field plots constitute a plot design with a long history in forest inventory which
37 is part of the plot design of most national forest inventories. In the early 19th century at the latest
38 – and long before statistical sampling had been established, the then called “representative
39 method” (Kiaer 1895-96) - fixed area plots were used to expand plot observations to entire
40 stands (e.g. König 1835, Heyer 1861). When sampling for tree attributes, there are at least two
41 different views on fixed area plots each of which carries a different analysis approach: (1) The
42 plot cuts out a sample area from a population (defined as the horizontally projected surface of
43 a defined area of forest land) with recordings of all observations exactly above that area; this
44 may be individual objects but also a continuously distributed variable (henceforth, we call this
45 approach the “continuous approach”, CA); and (2), the plot serves as a selection tool and defines
46 the discrete set of sample trees to be included into this particular plot from the population of all
47 trees in a defined area of forest land (we will call this approach the “discrete approach” DA in
48 what follows). In CA, the per-plot observation is the total of the target variable exactly above
49 the horizontal projection of the plot area (for circular plots, the biomass within a cylinder on

50 the plot perimeter), and in DA the per-plot observation comes from the total of the target
51 variable over all included sample objects (trees). In remote sensing, the CA is the natural
52 approach when the plot area is matched as well as possible with the image data (pixels). Naesset
53 (2002) called it the “area based approach” (ABA), which, in remote sensing is contrasted to the
54 “individual tree detection” approach. In field sampling, it is commonly the DA which is applied,
55 with a recording of tree variables for all sample trees on the plot, regardless of whether a sample
56 tree has parts of its stem and crown outside the plot area. Both approaches CA and DA and their
57 corresponding different analysis approaches have been applied in plot design comparisons
58 when sampling for dead wood: Gove and Van Deusen (2011) introduced the instructive terms
59 “chainsaw method”, when only those parts of the deadwood are recorded that are exactly above
60 the plot area (as if cut out by a chainsaw; this corresponds to our CA), and “stand-up method”,
61 when all those deadwood pieces with their thicker end within the plot area are included and
62 recorded (as if these dead wood pieces would stand up within the plot; this corresponds to our
63 DA). In forest inventory field sampling, both approaches may be applied and they differ in
64 efforts and in precision of estimation while for both, unbiased estimators are available.

65 To the best of our knowledge, these two approaches have not been compared for other
66 variables than dead wood, and certainly not for above ground biomass, which has become a
67 core variable in forest monitoring. The role of forests in the global carbon cycling accentuates
68 the importance of quantifying both state and trends in forest biomass (IPCC 2006) and points
69 to the demand for altogether “credible” estimates: for forest biomass and carbon monitoring,
70 the Conference of the Parties (COP) to the UN-Climate Convention (UN-FCCC) explicitly
71 requests the countries (Parties to the Convention) to establish “A robust and transparent national
72 forest monitoring system ...”; and these monitoring systems should “Provide estimates that are
73 transparent, consistent, as far as possible accurate, and that reduce uncertainties” (UNFCCC

74 COP decisions 4/CP.15, 1/CP.16, 9/CP19). That is: there is an important call to investigate
75 opportunities for improvements of precision of forest biomass estimation; as we do it here.

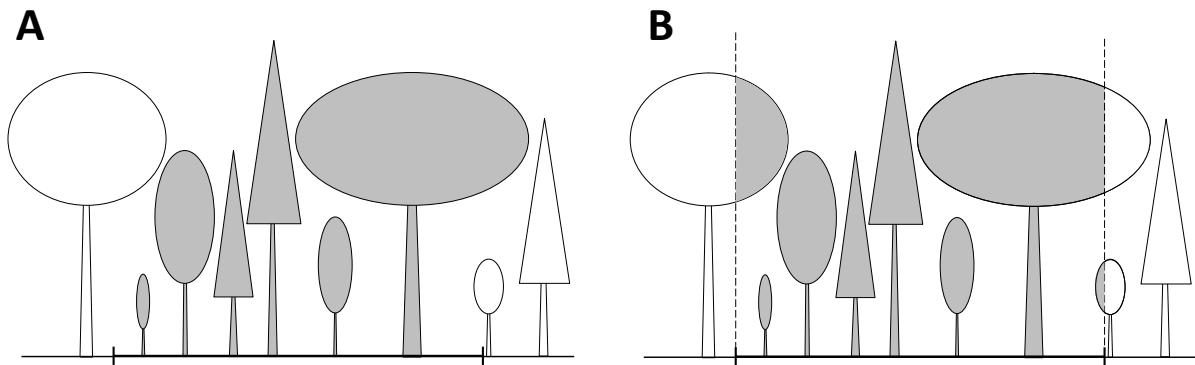
76 Above ground biomass is defined as “all living biomass above the soil including stem,
77 stump, branches, bark, seeds and foliage” (IPCC 2006). To bypass issues of destructive biomass
78 sampling, tree biomass is predicted with models linking biomass to easy-to-measure tree
79 variables, in particular the diameter at breast height (*dbh*) given its correlation with stem basal
80 area, and tree height (Brown et al. 1989, Fehrmann et al. 2008, Picard et al. 2012, Chave et al.
81 2015, Magnussen and Carillo Negrete 2015). Most tree biomass models only predict the above
82 ground component of the live biomass, while below ground biomass is commonly determined
83 by simple conversion factors (as e.g. in IPCC 2006).

84 In this study, we compare the precision of estimation of AGB from fixed area field
85 inventory plots under the two approaches CA and DA. The DA is the textbook approach to
86 plot-level biomass observation and estimated as the sum over the trees in a plot from the
87 biomass predicted for each tree using an appropriate model (Kershaw et al. 2016). A DA
88 estimate of plot-level biomass may also include crown parts of sample trees that extend outside
89 the plot perimeter or biomass in oblique stems leaning outside the plot area.

90 We consider the continuous approach (CA) that looks at tree biomass as a variable that is
91 continuously distributed horizontally. Its application requires for each inventory plot a
92 prediction of the continuous horizontal biomass distribution (HBD) since the biomass is
93 determined strictly above the plot area. A continuous view is also adopted in forest monitoring
94 when defining an infinite population of sample elements (plots) in an area sampling frame
95 (Mandallaz 1991), but extending a continuous view to inventory variables is new; to the best of
96 our knowledge, modelling a continuous distribution of a tree related variable (here: biomass)
97 to produce plot-level observations of such variable has not been reported before. Outside forest

98 inventories, a continuous view is not uncommon, like, for example, topographic variables such
99 as height above sea level, and remotely sensed crown surfaces.

100 Figure 1 illustrates the key difference between DA and CA for the estimation of AGB.



101
102 **Figure 1.** Schematic comparison of (A) the discrete approach DA and (B) the continuous
103 approach CA to determining plot-level biomass. The plot size is represented by the bold black
104 line at ground level, and for the CA, the vertical dashed lines mark the positions between which
105 the biomass is considered.

106
107 While the vertical distribution of forest biomass has been researched intensively (e.g. Nemeč
108 et al. 2012, Jiménez et al. 2013, Ruiz-González and Álvarez-González 2011, Tahvanainen and
109 Forss 2008), studies that address the horizontal forest or tree biomass distribution are sparse.
110 Kershaw and Maguire (1996) and Xu and Harrington (1998), modelled the horizontal
111 distribution of leaf biomass - but not AGB. Affleck et al. (2012) also noted an absence of
112 HBDs for modelling of fuel load where HBDs would be required to take full advantage of
113 next-generation fire behaviour simulators, and to improve fuel management strategies to
114 reduce fire hazard. Mascaro et al. (2011) considered a uniform HBD across the crown
115 projection area in a study on uncertainty of carbon estimation and may have been the first to
116 work the DA/CA issue in the context of airborne laser scanning (ALS) for forest carbon. They
117 named the approaches “stem-localized” (corresponding to our DA and Gove’s and Van
118 Deusen’s (2011) “stand-up” approach) and “crown-distributed” (corresponding to our CA and

119 Gove and Van Deusen’s (2011) “chainsaw” method). Mascaro et al. (2011) investigated the
 120 issue within in a remote-sensing based modelling context. Their main finding was that
 121 RMSEs were lower for the “crown-distributed” approach when modelling biomass from ALS
 122 data. As expected, the results varied with field plot size.

123 This study is a first step towards integrating the horizontal distribution of forest biomass
 124 into AGB estimation from forest inventory field sampling. To that end, we provide a case study
 125 where DA estimates of AGB are compared to CA estimates derived by considering AGB as a
 126 continuous variable across an area of interest. This case allows us to draw first conclusions
 127 about the CA’s statistical performance, and identify pathways for further developments.

128

129 **2. Materials and methods**

130 *2.1. Study area*

131 Data for our simulations come from a two ha (100 m × 200 m) area within a stand dominated
 132 by beech (*Fagus sylvatica* L., 92.3% in both basal area and number of trees) near Göttingen,
 133 Germany (51°33'52.3"N 9°57'53.8"E). The stand was fully tallied: for each tree, species was
 134 identified and its *dbh* (cm) measured with a tape to the nearest millimeter. Summary statistics
 135 are in Table 1.

136

137 **Table 1.** Characteristics of the 2ha study area. *N* = stand density, *G* = basal area, and *dg* =
 138 quadratic mean diameter.

	Total	Beech	Other Broadleaves	Conifers
<i>N</i> (trees·ha ⁻¹)	183.0	169.0	9.0	5.0
<i>G</i> (m ² ·ha ⁻¹)	25.1	23.1	0.9	1.1
<i>dg</i> (cm)	41.8	41.7	35.7	54.1

139

140 Tree heights and maximum crown diameters (CD_{max} = diameter of crown projection
141 area) were predicted from dbh via local models (Guericke, 2001). The crown projection for a
142 tree is assumed circular.

143

144 *2.2 Construction of a tree-level HBD*

145 The cornerstone in the CA is a tree specific HBD for all trees in a plot, and for trees outside the
146 plot with a biomass from branches and foliage inside the plot perimeter. The HBD distributes
147 a predicted tree biomass over a tree's crown projection area.

148 Mascaro et al. (2011) proposed a uniform distribution assigning, unrealistically, the same
149 biomass density to the inner and outer parts of a tree crown. To improve realism, we develop a
150 per-tree crown horizontal biomass distribution by combining a simple model for the stem with
151 models for branch-wood, and foliage biomass derived from allometry, and horizontal foliage
152 distribution.

153 First, we predicted the AGB for each tree separately for the compartments stem, branches
154 and foliage with models provided in Bartelink (1997). Next, we addressed the spatial
155 distribution of each biomass component across a horizontally projected crown area: for the stem
156 biomass, we assumed a distribution within the confinements of a cone (centered at the tree
157 position) with a basal diameter (BD) at ground level (height zero) predicted from the dbh
158 (assuming a cone shape) and tree height..

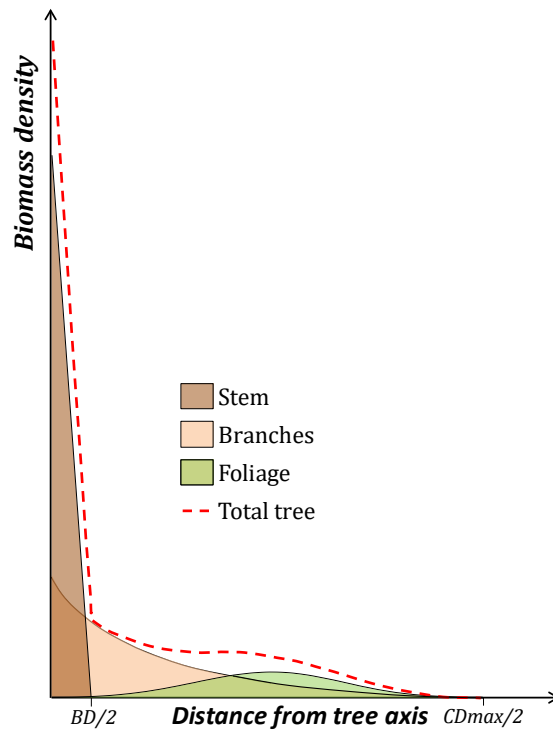
159 To predict branch biomass at a given distance from the stem center we used models
160 developed by Pérez-Cruzado et al. (in preparation) for beech from nearby the study stand. The
161 branch biomass at a given distance from the stem center was estimated using a model proposed
162 by Max and Burkhardt (1976) for stem taper:

$$wb = \left(-0.0047 \cdot (RCR - 1) + 0.0024 \cdot (RCR^2 - 1) + 0.0366 \cdot (0.6654 - RCR)^2 \right. \\ \left. \cdot \frac{\max((0.6654 - RCR), 0)^{0.5}}{(0.6654 - RCR)} \right) + \varepsilon \quad [1]$$

163 where wb is the standardized branch biomass density at the relative crown radius RCR
 164 ($RCR=CR_i/CDmax_i/2$) for the tree i ; and ε is a random error term. Thus branch biomass is
 165 assumed to decrease with the distance to the center of the stem. At a distance of $CDmax/2$ the
 166 branch biomass density approaches zero (Figure 2).

167 The horizontal distribution of foliage biomass is modelled as three-parameter Weibull
 168 probability density function. This approach has been previously used to characterize horizontal
 169 distribution of foliage for different species and crown positions (e.g. Kershaw and Maguire,
 170 1996; Xu and Harrington 1998). We chose a location parameter equal to 0, a scale parameter
 171 of 0.61, and a shape parameter equal to 3.55. These parameter values base on a study in
 172 preparation (Pérez-Cruzado, in preparation)

173



175 **Figure 2.** Schematic profile of the horizontal distribution of stem, branches, foliage biomass,
 176 and combined (AGB) in an individual tree and arbitrary direction. BD is the basal diameter of
 177 the stem, derived from dbh (assuming cone shape); CD_{max} is the maximum crown diameter.

178

179 The 3D HBD for each biomass component (stem, branches and foliage) was generated by
 180 rotating the corresponding functions around the stem axis. We standardized the X axis of the
 181 distribution (distance from the tree axis in Fig. 2) to the $CD_{max}/2$ of each tree, and equated the
 182 volume under the rotation solid over the horizontal plane. Hence, we assume that the HBD is
 183 isotropic in the horizontal plane and we assume the same standardized distribution for all trees.
 184 Figure 2 illustrates the horizontal profile distribution of biomass for a tree with known crown
 185 diameter CD_{max} , DBH and $height$.

186

187

188 *2.3 Construction of an area-level HBD*

189 To illustrate the difference between AGB estimates from DA and CA for an area of interest, we
190 need an HBD model for the entire area (here: our 2 ha study area). In principle this is done by
191 predicting the HBD for each tree and adding these predicted biomasses for each location in the
192 study area. To be practical, we chose to rasterize the study area into cells of $2\text{ cm} \times 2\text{ cm}$
193 (resulting in a total of 50×10^6 cells). The high spatial resolution of the horizontal distribution
194 of biomass over the study area provides an approximation to the continuous biomass
195 distribution.

196 To facilitate a comparison between DA and CA estimates of AGB, and to better illustrate
197 their differences, we also produced an HBD model for the study area as it would emerge with
198 the DA. In contrast to CA, the DA specific HBD model assigned the predicted AGB of a tree
199 to the single $2\text{ cm} \times 2\text{ cm}$ cell containing the stem position; resulting in a HBD map where the
200 biomass values are concentrated at the tree positions in peaks whose height depends on the
201 respective tree's biomass.

202 The DA and CA area-level HBD models are used next in a sample simulation as a basis
203 for comparison.

204

205 *2.4 Sample simulation*

206 To capture effects of plot-size and shape, we carried out simulations with two common plot
207 shapes (circles as preferred in forest inventory and squares as preferred in ecological surveys),
208 and 17 plot sizes (100, 200, ..., 1700 m²). As our DA-CA comparison should not be influenced
209 by Monte-Carlo errors (Koehler 2009) we opted for simulating all possible samples through the
210 construction of a sampling surface (Van Deusen et al. 1986, Roesch et al. 1993, Hradetzky

211 1995). A sampling surface is specific to a plot design, and provides - for each point within a
212 defined sampling frame (area) - the AGB value that would be realized (from either a DA or CA
213 HBD area level model) had the point been selected for sampling. Our sampling frame was the
214 grid with the total of 50×10^6 square units of 4 cm^2 . Upon completion we have, for each plot
215 design, two sampling surfaces of AGB, one for DA, and one for CA.

216 In our simulations we eliminated boundary effects by excluding sample locations with a
217 distance less than or equal to 23.26 m from a study area border. The width of this sample
218 exclusion zone corresponds to the radius of the largest circular plot. In actual applications,
219 boundary effects will be different for DA and CA, but they are beyond the scope of our study.

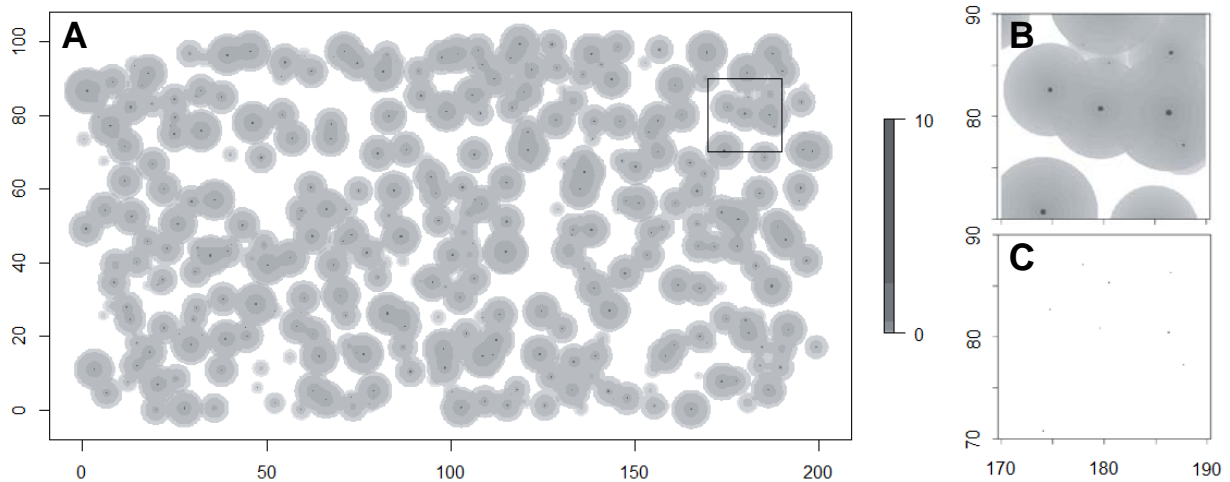
220 The standard deviation of all AGB values across all 4 cm^2 units in a sampling surface for
221 a specific plot design and approach (DA or CA), is an estimator of the expected standard error
222 under simple random sampling and a sample size of $n = 1$. Standard errors for larger sample
223 sizes are not needed; they are covered by the central limit theorem (Johnson 2004).

224 To illustrate our results also in more practical terms, we defined a target relative sampling
225 error of 5% and compared the expected sample sizes required to reach this target with DA and
226 CA under the various plot designs. All statistical analyses and computations were made in R (R
227 Core Team, 2018).

228

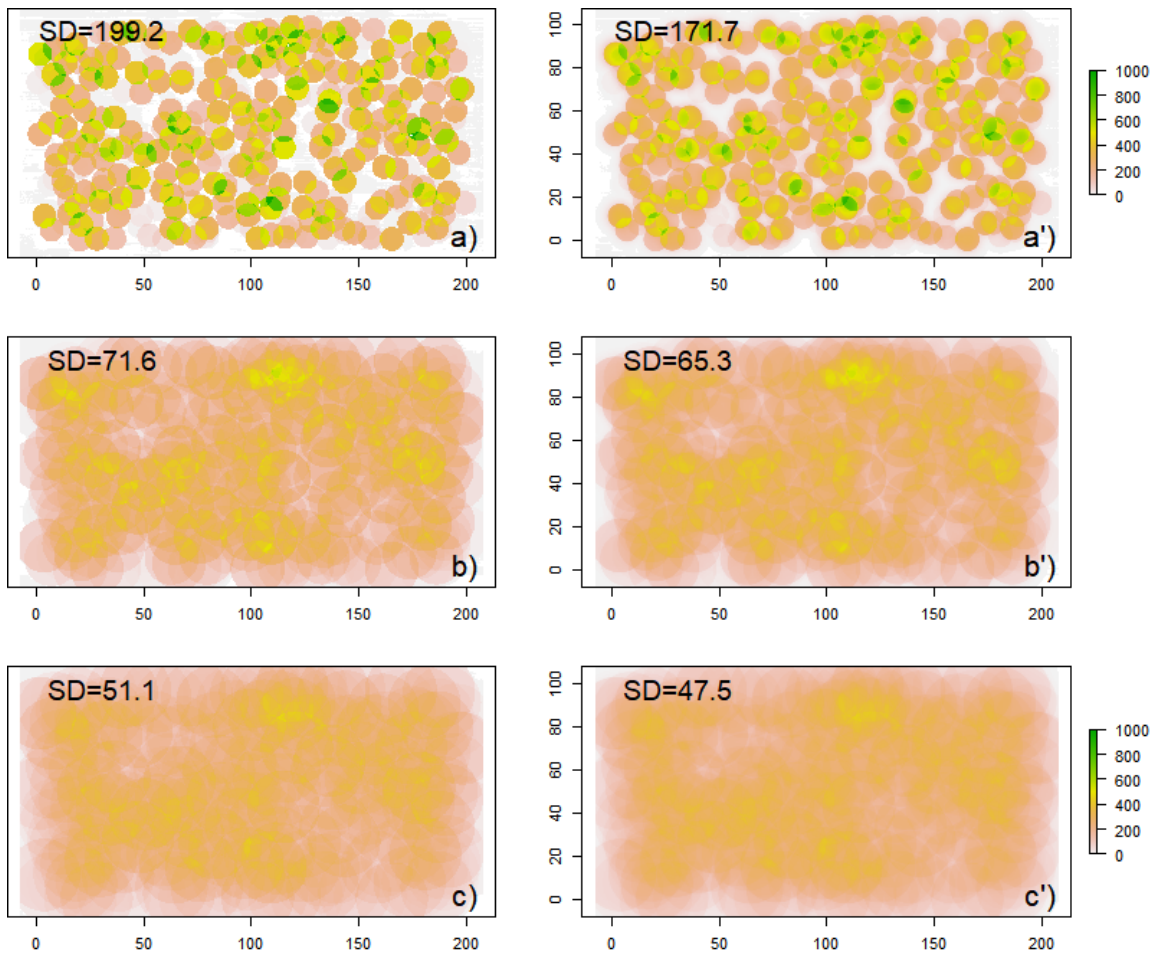
229 **3. Results**

230 We first build the HBDs for the study area for both approaches, CA and DA. The enlarged 20
231 m x 20 m sections in Figure 3 illustrate the difference between the two, where the biomass
232 distribution for DA is characterized by high peaks at the tree positions while under CA the tree
233 biomass is distributed over each crown area isotropically as per our example in Figure 2.



234
 235 **Figure 3.** Horizontal above ground biomass distribution for all tree components (stem +
 236 branches + foliage) for CA (maps A and B) and DA (map C). Map A shows to the entire 2 ha
 237 study area. Maps B and C amplify the 20 m × 20 m square shown in map A. The units of the
 238 grey values are “kg per 4 cm² cell” (raster cell of 2 cm x 2 cm).
 239

240 From the HBD of the study stand we calculated the AGB sampling surfaces both for the
 241 DA and the CA (Figure 4, [Mg·ha⁻¹]). A sampling surface is specific for a defined plot design
 242 and gives per point (cell of 2 cm × 2cm) the per-plot biomass value that results for a sample
 243 plot centred at this particular point. While the topography of a sampling surface map varies by
 244 the two approaches and by plot design, the overall mean of ABG computed for the sampling
 245 frame of 4 cm² units remains almost constant at 279.25 Mg·ha⁻¹. As expected, for a given plot
 246 size, the sampling surfaces (Figure 4) are smoother for the HBD of the CA than for the HBD
 247 of the DA. Equally, these differences diminish with an increase in plot size due to a lowering
 248 of the within-surface variance. In plot sizes above 900m² the difference in the smoothness of
 249 the DA and the CA sampling surface were minor and without practical importance (not shown).
 250

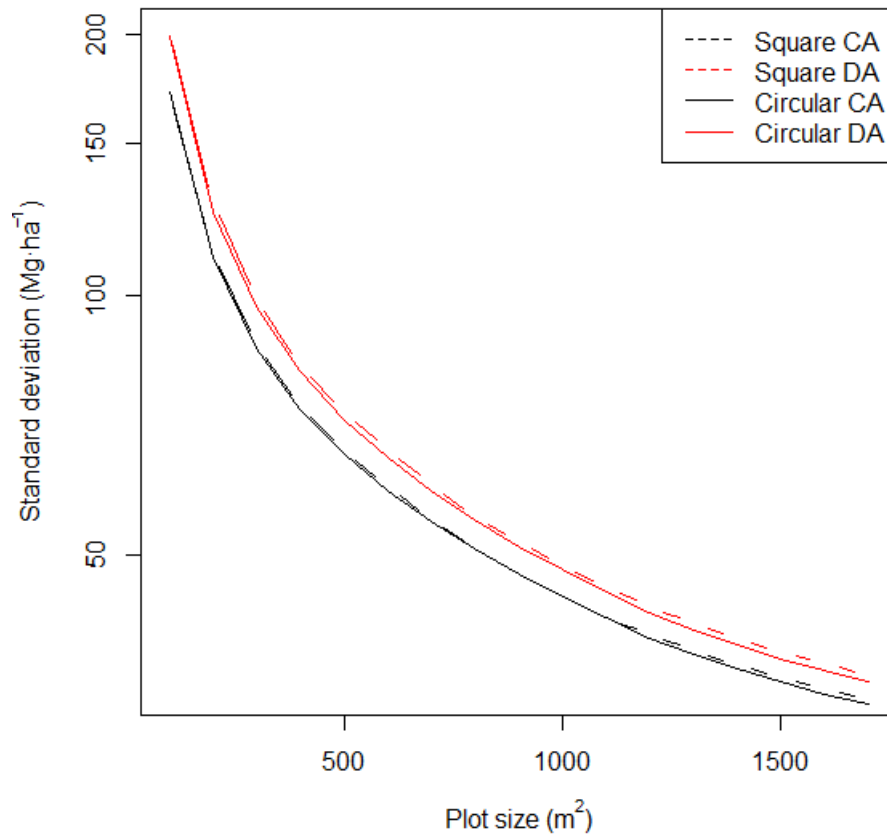


251 **Figure 4.** Sampling surfaces for the DA (left, a-c) and the CA (right, a'-c') approaches for
 252 estimation of AGB with a circular plot with an area of: 100m² (a, a'); 500m² (b, b'); and 900m²
 253 (c, c'). The color scale illustrates the values of the observed plot-level biomass in Mg·ha⁻¹ and
 254 SD is the standard deviation (Mg·ha⁻¹) of surface values of AGB.

255

256 A smoother (less variable) sampling surface translates to a lower standard error in a mean
 257 estimated from a probability sample. Figure 5 graphs the standard deviations of the DA and CA
 258 HBD sampling surfaces by plot size. The CA sampling surface has consistently a smaller
 259 standard deviation for all plot sizes and the two plot shapes (circular, square). The relative
 260 reduction in variability is more pronounced for smaller plots and decreases as plot size is
 261 increased. This can be explained by a higher perimeter-to-area ratio of a smaller plot, so that
 262 per unit area, the frequency of crowns intersecting a smaller plot is higher than for a larger plot.

263 Figure 5 also indicates a (small – but consistently) superior performance of the circular plot
264 shape, a feature in line with the minimum perimeter-to-area ratio of a circle.

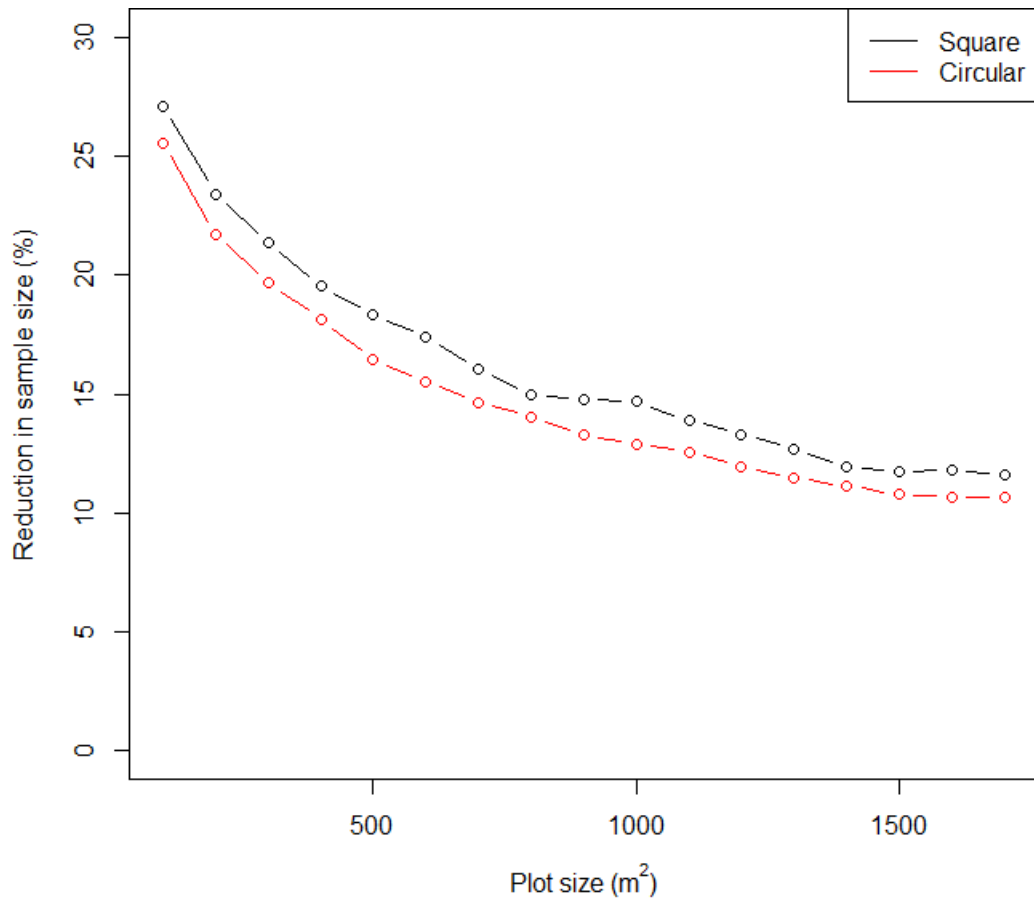


265 **Figure 5.** Standard deviation (log scale) of the DA and CA sampling surfaces of AGB as a
266 function of plot area (and shape). Differences between square and circle shape are small, but
267 CA produces clearly lower standard deviations.

268

269 We also used the DA and CA sampling surfaces of plot-level AGB estimates to gauge the
270 required sample size for a target relative standard error of 5% in an estimate of the mean AGB
271 in the studied sample frame. The results are in Figure 6. As alluded to, the CA can achieve the
272 target with a smaller sample size. In our study area, a reduction of 27.1 % was achieved with
273 our smallest plots of 100 m². For the largest plots considered (1,700 m²), the reduction was

274 10.4%. We noted a slightly but consistent greater (1.4%) reduction with circular plots than with
275 square plots, in agreement with their more favourable perimeter-to-area ratio.



276

277 **Figure 6.** For the 2 ha study area: reduction in required sample size as a function of plot area
278 for the DA and the CA, for a defined target standard error of 5% in AGB.

279

280

281 **4. Discussion**

282 For field sampling, our case study indicates that the CA approach to estimation of AGB
283 tends to be more efficient in terms of precision of estimation than the traditional DA. This
284 advantage of CA over DA will depend however, in a rather complex ways, on tree species, tree
285 and crown sizes, stand structures, stem densities, and interactions of these factors with plot size
286 and shape (in particular perimeter length). In our case study, for a defined target precision of
287 estimation, we observed a reduction of required sample size of about 10 % for larger plots
288 (1700m²) and about 27 % for small plots (100m²). It will be instructive to look in more detail
289 into the factors influencing this gain in precision.

290 We may compare our findings regarding the precision of estimation with those of a dead
291 wood sampling study by Gove and Van Deusen (2011), who compared the performance of their
292 “stand-up method” (corresponding to our DA) to their “chainsaw method” (corresponding to
293 our CA) to estimate the volume of downed coarse woody debris. They found the CA to be
294 superior: in their study, the standard deviations for the sample surfaces were 135.48 m³ and
295 120.18 m³, respectively so that their (continuous) chainsaw approach was approximately 12 %
296 more precise than the (discrete) stand-up approach. Mascaro et al (2011) did also observe
297 superiority of their version of the CA when they derived a remote sensing-based model for
298 forest biomass prediction.

299 For this first of its kind case study on the comparison of the CA and the DA, we needed
300 to work with various simplifying assumptions regarding regular and symmetric (rotational)
301 stem and crown shapes, branch allometry, profile distributions of foliage, an isotropic
302 distribution of biomass within the volumetric confinements of a biomass component, and
303 perfectly upright stem axes. Combined, these assumptions may have impacted the results of our

304 sampling study. Refinements are clearly needed, and in light of our results we will pursue
305 improvements in the next iteration. At any rate, it will be important to research if using more
306 realistic models for each biomass component will significantly change the performance
307 differential between CA and DA.

308 From a practical perspective, the DA method for estimation of AGB has well-established
309 advantages in terms of expediency because measurements and model-based predictions are
310 straightforward and apply only to the sample trees within a plot. With the DA, there is neither
311 need for a map of tree locations in the plot nor measurements (*dbh* and location) of trees in the
312 surrounding vicinity of a plot as required by the CA. It is obvious, that additional measurements
313 come at a cost detrimental to existing budgets to support already costly field work. However,
314 one may realistically expect the near future to bring us forest mensuration devices that allow to
315 automatically and simultaneously measure the distance to sample trees, the height 1.3m and the
316 diameter there. This would speed up field work on mapped forest inventory plots and their
317 surrounds and render practical applications of the CA approach more attractive.

318 We compared DA and CA from a perspective of field plot sampling only. The theoretical
319 consistency of the CA in terms of estimating AGB over a specifically defined piece of forest
320 (the plot area) is particularly important in model assisted and model-based estimation problems
321 in which remotely sensed auxiliary variables are linked to per-plot values of AGB (Nelson et
322 al. 2000, Mascaro et al 2011, Magdon et al. 2018). Conceptually, the remotely sensed auxiliary
323 variable only registers the biomass within the confinements of a field plot while the field data
324 from the DA include biomass of plot trees extending beyond the plot perimeter, and ignore the
325 biomass from outside trees overhanging a plot. The extent of the misalignment depends (to a
326 large degree) on the spatial resolution or density of the remotely sensed data, plot size and in
327 particular plot perimeter. In cases where the spatial resolution is much finer than the size of
328 most crown areas, the CA approach should, *a priori*, tend to generate a stronger correlation

329 between the auxiliaries in an assisting model and AGB than possible with DA because the
330 misalignment of biomass vis-à-vis the confinements of a plot will act as a measurement
331 error - with an attenuation of correlations (Fuller 1987, Carroll 2006). In fact, Mascaro et al.
332 (2011) in their ALS study, addressed three major sources of errors: (1) GPS positional error,
333 (2) temporal differences between the field and LiDAR data, and (3) a lack of consistency
334 between LIDAR and field plot measurements rooted in the uncertainty of deciding on whether
335 a tree or a tree part resides inside the confinements of a field plot. With respect to the third
336 source of error, which relates to our study, they found that the root mean square error (RMSE)
337 of the model that links the LiDAR with the ground data could be consistently improved with a
338 CA approach replacing the traditional DA. This ‘third’ error has so far not been explicitly
339 recognized in otherwise detailed error budgets for AGB estimates in forest monitoring (Chave
340 et al. 2004, Ståhl et al. 2014, Molto et al. 2013, Magnussen et al. 2014, Chen et al. 2016).

341

342 **5. Conclusions**

343 Our overall goal was to contribute to improving the precision of forest biomass estimation
344 from field sampling, as the standard error constitutes a relevant source of uncertainty in many
345 monitoring programs for forest biomass, notably in national forest inventories with their large
346 sample sizes. On that note, we may conclude that CA has the potential to improve the precision
347 of field estimated AGB. However, the CA approach is unlikely to be operational until issues
348 related to field measurement efforts can be resolved. Moreover, the inroad of CA in forest
349 inventory will not only depend on the availability of measurement devices for rapid mapping
350 of trees around a sample point, recordings of *dbh* and delineation of crown projection areas, but
351 also on an expansion of our arsenal of models for crown sizes, foliage distribution, and branch
352 architectures.

353

354 **References**

- 355 Affleck, D.L.R., Keyes, C.R., Goodburn, J.M. 2012. Conifer crown fuel modeling: Current
356 limits and potential for improvement. *West. J. Appl. For.* 27, 165-169.
- 357 Bartelink, H.H. 1997. Allometric relationships for biomass and leaf area of beech (*Fagus*
358 *sylvatica* L). *Ann. For. Sci.* 54, 39-50.
- 359 Brown, S., Gillespie, A., Lugo, A.E. 1989. Biomass Estimation Methods for Tropical Forests
360 with Applications to Forest Inventory Data. *Forest Science* 35(4):881-902.
- 361 Brown, S., 1997. Estimating biomass and biomass change of tropical forests – a primer. FAO
362 Forestry Paper 134. 55p.
- 363 Carroll, R.J. et al. 2006. Measurement error in nonlinear models: A modern perspective.
364 Chapman & Hall / CRC Press. 484p.
- 365 Chave, J., Condit, R., Aguilar, S., Hernandez, A., Lao, S., Perez, R. 2004. Error propagation
366 and scaling for tropical forest biomass estimates. *Philosophical Transactions of the Royal*
367 *Society of London. Series B: Biological Sciences* 359(1443):409-420.
- 368 Chave J., Rejou-Mechain, M., Burquez, A., Chidumayo, E., Colgan, M.S. Delitti, W.B.C.,
369 Duque, A., Eid, T., Fearnside, P.M., Goodman, R., Henry, M., Martinez-Yrizar, A.,
370 Mugasha, W.A., Muller-Landau, H.C. , Menuccini, M., Nelson, B.W., Ngomanda, A.,
371 Nogueira, E.M., Ortiz-Malavassi, E., Pelissier, R., Ploton, P., Ryan, C.M., Saldarriaga,
372 J.G., Vielleedent G. 2015. Improved allometric models to estimate the above ground
373 biomass of tropical trees. *Global Change Biology* (2015) 20, 3177–3190.
- 374 Chen Q., McRoberts, R.E., Wang, C., Radtke 2016 Forest aboveground biomass mapping and
375 estimation across multiple spatial scales using model-based inference. *Remote Sensing of*
376 *Environment* 184 (2016) 350–360
- 377 Enquist, B.J. 2002. Universal scaling in tree and vascular plant allometry: toward a general
378 quantitative theory linking plant form and function from cells to ecosystems. *Tree Physiol.*
379 22, 1045-1064.
- 380 Fehrmann L., Lehtonen, A., Kleinn, C., Tomppo, E. 2008. Comparison of linear and mixed-
381 effect regression models and a k-nearest neighbour approach for estimation of single-tree
382 biomass. *Canadian Journal of Forest Research* 38(1): 1-9.
- 383 Fuller, W.A. 1987. Measurement error models. Wiley, New York. 440p.

384 Gove, J.H., Van Deusen, P.C. 2011. On fixed-area plot sampling for downed coarse woody
385 debris. *Forestry* 84, 109-117.

386 Guericke, M. 2001. Growth dynamics of mixed stands of Beech and European Larch (*Larix*
387 *decidua*, Mill.). Georg August Universität Göttingen 273.

388 Hradetzky, J. 1995. Concerning the precision of growth estimation using permanent
389 horizontal point samples. *For. Ecol. Manage.* 71, 203-210.

390 Heyer G. 1861. Notizen: A. Über die Größe der Probeflächen (in German: Notes: A. About
391 the size of sample plots). *Allgemeine Forst- und Jagdzeitung AFJZ*. Oktober 1861:399.

392 IPCC. 2006. Guidelines for National Greenhouse Gas Inventories. [https://www.ipcc-](https://www.ipcc-nggip.iges.or.jp/public/2006gl/vol1.html)
393 [nggip.iges.or.jp/public/2006gl/vol1.html](https://www.ipcc-nggip.iges.or.jp/public/2006gl/vol1.html)

394 Jiménez, E., Vega, J.A., Ruiz-González, A.D. , Guijarro, M., Alvarez-González, J.G.,
395 Madrigal, J., Cuiñas, P., Hernando, C., Fernández-Alonso, J.M. 2013. Carbon emissions
396 and vertical pattern of canopy fuel consumption in three *Pinus pinaster* Ait. active crown
397 fires in Galicia (NW Spain). *Ecol. Eng.* 54:202-209.

398 Johnson, O. T. 2004. Information Theory and the Central Limit Theorem. Imperial College
399 Press. 88p.

400 Kershaw, J.A., Maguire, D.A. 1996. Crown structure in western hemlock, Douglas-fir, and
401 grand fir in western Washington: trends in branch-level mass and leaf area. *Can. J. For.*
402 *Res.* 25, 1897-1912.

403 Kershaw, J.A., Ducey, M.J., Beers, T. W., Husch, B. 2016. *Forest Mensuration*. 5th edition.
404 Wiley-Blackwell. 630p.

405 Kiaer AN. 1895-96. Observations et expériences concernant des dénombrements
406 représentatives. *Bulletin of the International Statistical Institute*, IX, Book 2: 176-183.

407 König G. 1835. *Forstmathematik* (in German: "Forest Mathematics"). Gotha, in Commission
408 der Beckerschen Buchhandlung. 436p. + 56p of tables (2nd edition 1854).

409 Koehler, E., E. Brown, and J.-P.A. Haneuse. 2009. On the assessment of Monte Carlo error in
410 simulation-based statistical analyses. *Am. Stat.* 63(2):155-162.

411 Magdon, P., González-Ferreiro, E., Pérez-Cruzado, C., Purnama, E.S., Sarodja, Y., Kleinn, C.
412 2018. Evaluating the Potential of ALS Data to Increase the Efficiency of Aboveground
413 Biomass Estimates in Tropical Peat-Swamp Forests. *Remote Sensing* 10 (9), 1344.

414 Magnussen, S., M. Köhl, K. Olschofsky. 2014. Error propagation in stock-difference and
415 gain–loss estimates of a forest biomass carbon balance. *Eur. J. For. Res.* 133(6):1137-1155.
416 DOI: 10.1007/s10342-014-0828-0

417 Magnussen, S., Carillo Negrete, O.I. 2015. Model errors in tree biomass estimates computed
418 with an approximation to a missing covariance matrix. *Carbon Balance Manag.* 10: 21.

419 Mandallaz, D. 1991. A unified approach to sampling theory for forest inventory based on
420 infinite population and superpopulation models [online]. *Diss. Techn. Wiss. ETH Zürich*
421 9378.

422 Mascaro, J., Detto, M., Asner, G.P., Muller-Landau, H.C. 2011. Evaluating uncertainty in
423 mapping forest carbon with airborne LiDAR. *Remote Sens. Environ.* 115, 3770-3774.

424 Max, T.A., Burkhart, H.E., 1976. Segmented polynomial regression applied to taper
425 equations. *For. Sci.*22, 283-289.

426 McRoberts, R.E., Næsset, E., Saatchi, S., Liknes, G.C., Walters, B.F. Chen, Q. 2019. Local
427 validation of global biomass maps. *International Journal of Applied Earth Observation and*
428 *Geoinformation*. Volume 83, November 2019, 101931.

429 Molto, Q., V. Rossi, L. Blanc. 2013. Error propagation in biomass estimation in tropical
430 forests. *Methods in Ecology and Evolution* 4(2):175-183. 10.1111/j.2041-
431 210x.2012.00266.x

432 Montero, G., Ruiz-Peinado, R., Nuñez, M. (2005). Producción de biomasa y fijación de CO₂
433 por los bosques españoles. *Monografías INIA. Serie Forestal* nº 13. 270 pp.

434 Næsset, E., 2002. Predicting forest stand characteristics with airborne scanning laser using a
435 practical two-stage procedure and field data. *Remote Sens. Environ.* 80, 88–99.
436 doi:10.1016/S0034-4257(01)00290-5

437 Nemec, A.F.L., Parish R., Goudie, J.W. 2012. Modelling number, vertical distribution, and
438 size of live branches on coniferous tree species in British Columbia. *Can. J. For. Res.*
439 42(6):1072-1090.

440 Nelson, R., Jimenez, J., Schnell, C. E., Hartshorn, G. S., Gregoire, T. G., Oderwald, R. 2000.
441 Canopy height models and airborne lasers to estimate forest biomass: Two problems.
442 *International Journal of Remote Sensing* 21:2153–2162.

443 Pérez-Cruzado, C., Merino, A., Rodríguez-Soalleiro, R. 2011. A management tool for
444 estimating bioenergy production and carbon sequestration in *Eucalyptus globulus* and
445 *Eucalyptus nitens* grown as short rotation woody crops in north-west Spain. *Biomass and*
446 *Bioenergy* 35:2839-2851.

447 Pérez-Cruzado, C., Nölke, N., Magdon, P., Álvarez-González, J.G., Fehrmann, L., Kleinn, C.
448 In preparation. The horizontal distribution of branch biomass of European beech: a TLS
449 study with subsequent destructive measurements. *Remote Sensing*.

450 Picard, N., Saint-André, L., Henry, M. 2012. Manual for building tree volume and biomass
451 allometric equations - From field measurement to prediction. CIRAD et FAO. 215p.

452 R Core Team. 2018. R: A Language and Environment for Statistical Computing. R
453 Foundation for Statistical Computing.

454 Roesch, F.A., Green, E.J., Scott, C.T. 1993. An alternative view of forest sampling. *Surv.*
455 *Methodol.* 19, 199-204.

456 Ruiz-González, A.D., Álvarez-González, J.G. 2011. Canopy bulk density and canopy base
457 height equations for assessing crown fire hazard in *Pinus radiata* plantations. *Can. J. For.*
458 *Res.* 41(4):839-850.

459 Schepaschenko, D. and 144 co-authors. 2019. The Forest Observation System, building a
460 global reference dataset for remote sensing of forest biomass. *Nature | Scientific Data*
461 6:198.

462 Ståhl G., Heikkinen J., Petterson, H., Repola J., Holm S. 2014. Sample-Based Estimation of
463 Greenhouse Gas Emissions From Forests—A New Approach to Account for Both
464 Sampling and Model Errors. *For. Sci.* 60(1):3–13.

465 Tahvanainen, T., Forss, E. 2008. Individual tree models for the crown biomass distribution of
466 Scots pine, Norway spruce and birch in Finland. *For. Ecol. Manage.* 255(3):455-467.

467 Tesfaye, M.A., Bravo-Oviedo, A., Bravo F., Ruiz-Peinado, R. 2016. Aboveground biomass
468 equations for sustainable production of fuelwood in a native dry tropical afro-montane
469 forest of Ethiopia. *Annals of Forest Science* 73:411–423.

470 UNFCCC COP decisions

471 4/CP.15: <https://unfccc.int/sites/default/files/resource/docs/2009/cop15/eng/11a01.pdf>

472 1/CP.16: <https://unfccc.int/sites/default/files/resource/docs/2010/cop16/eng/07a01.pdf>

- 473 9/CP19: <https://unfccc.int/sites/default/files/resource/docs/2013/cop19/eng/10a01.pdf>
- 474 Van Deusen, P.C., Dell, T.R., Thomas, C.E. 1986. Volume growth estimation from permanent
475 horizontal points. For. Sci.32, 415-422.
- 476 Xu, M., Harrington, T.B. 1998. Foliage biomass distribution of loblolly pine as affected by
477 tree dominance, crown size, and stand characteristics. Can. J. For. Res. 28, 887-892.
- 478

479 Declarations:

480 • Ethics approval and consent to participate

481 Not applicable

482

483 • Consent for publication

484 The authors confirm that they agree to publication of the manuscript

485

486 • Availability of data and material

487 Data and material will be made available upon reasonable request.

488

489 • Competing interests

490 There are no competing interests

491

492 • Funding

493 This study was entirely self-funded, no external funding.

494

495 • Authors' contributions

496 CK developed the idea, drafted the research design and wrote the first draft, CPC:

497 developed the models and programmed them. JGAG, PM: supported in programming and

498 writing; SM, LF, NN: supported implementation of the study, and data.

499 All authors critically participated in internal review rounds and read the final manuscript

500 and approved it.

501

502 • Acknowledgements

503 The authors will formulate an acknowledgement to the reviewers, then.

504